11-2022

In-vitro cell culture model to determine toxic effects of soil Arsenic due to direct dermal exposure

Manas Warke
Michigan Technological University, mwarke@mtu.edu

Madeline English
Michigan Technological University, mrenglis@mtu.edu

Laura De Marchi
Michigan Technological University, ldemarch@mtu.edu

Rohan Deep Sarkar
West Orange High School

Srinivas Kannan
Michigan Technological University, skannan1@mtu.edu

See next page for additional authors

Recommended Citation

Warke, M., English, M., De Marchi, L., Sarkar, R., Kannan, S., Datta, R., & Rao, S. (2022). In-vitro cell culture model to determine toxic effects of soil Arsenic due to direct dermal exposure. *Environmental Technology and Innovation, 28*. http://doi.org/10.1016/j.eti.2022.102949
Retrieved from: https://digitalcommons.mtu.edu/michigantech-p/16587

Follow this and additional works at: https://digitalcommons.mtu.edu/michigantech-p

 Part of the Biology Commons

Environmental Technology & Innovation 28 (2022) 102949

Contents lists available at ScienceDirect

Environmental Technology & Innovation

journal homepage: www.elsevier.com/locate/eti

In-vitro cell culture model to determine toxic effects of soil Arsenic due to direct dermal exposure

Manas Warke [a], Madeline English [b], Laura De Marchi [b], Rohan Deep Sarkar [c], Srinivas Kannan [b], Rupali Datta [a,d,e,*], Smitha Rao [a,b,d,e,*]

[a] Department of Biological Sciences, Michigan Technological University, 1400 Townsend Dr, MI, USA
[b] Department of Biomedical Engineering, Michigan Technological University, 1400 Townsend Dr, MI, USA
[c] West Orange High School, 51 Conforti Ave., West Orange, NJ, USA
[d] Great Lakes Research Center, Michigan Technological University, 1400 Townsend Dr, Michigan Technological University, MI, USA
[e] Health Research Institute, Michigan Technological University, 1400 Townsend Dr, Michigan Technological University, MI, USA

ARTICLE INFO

Article history:
Received 30 September 2022
Received in revised form 25 October 2022
Accepted 25 October 2022
Available online 2 November 2022

Keywords:
Soil Arsenic
In-vitro cell culture model
Arsenical-pesticides
Contact exposure

ABSTRACT

Arsenic (As) is one of the most toxic environmental pollutants, classified as a Class I carcinogen. Anthropogenic activities have led to an increase in As contamination of soils. Using animal models to study the health impacts of As is time and cost-prohibitive, hence attempts have been made to develop in-vitro cell culture models. However, most studies so far have not represented realistic environmental exposure conditions. We exposed Human Immortalized Keratinocyte (HaCaT) and Primary Human Dermal Fibroblasts (HDFa) cells to the water-soluble fraction of arsenic extracted from As spiked Immokalee soil to study the effect of soil As on skin cells. The impact of As was determined through cell viability, cell migration, and quantitative assessment of the expression of cadherins, CD44, and Zeb1 using Western Blotting and In-cell Western. Our data indicated that HaCaT cells were more susceptible to As-induced cellular transformation than HDFa cells. At concentrations above 225 mg/kg of soil As, cellular responses were impacted, and changes in the expression of proteins were observed in HaCaT cells. The work presented here is a methodical approach to studying the impacts of toxic elements such as As through innovative cellular models using realistic environmental conditions, that can be readily adapted for different exposure pathways.

1. Introduction

Arsenic (As) is a group I human carcinogen found in trace quantities in air, water, and soil (Benipal et al., 2017). Chronic exposure to As increases the risk of cancer of the bladder, lungs, kidneys, and liver (Straif et al., 2009). Arsenic exposure is also associated with the development of ischemic heart disease and peripheral vascular disease (Sodhi et al., 2019; Palma-Lara et al., 2020). Acute exposure has been associated with skin diseases such as keratosis and skin pigmentation (Pathania, 2021). The various natural and anthropogenic sources of As in soil include the biogeochemical decomposition of rocks and minerals, arsenical pesticides and herbicides, wood preservatives, and mining and smelting operations (Rakhimbekova et al., 2021). In the United States, the prolonged use of arsenical pesticides is evident in places such as the apple orchards

* Correspondence to: 1400 Townsend Dr, Houghton, MI 49931, USA.
E-mail addresses: rupdatta@mtu.edu (R. Datta), smithar@mtu.edu (S. Rao).

https://doi.org/10.1016/j.eti.2022.102949

of New Jersey, cotton fields in Texas, potato fields in Idaho, and cattle dipping sites in Florida. Although inorganic arsenical pesticides were banned in the 1980s, organic arsenical pesticides continued to be used as herbicides in agricultural lands and golf courses until they were banned in 2010 (Datta et al., 2006). The long-term use of arsenical pesticides has led to an increase in the concentration of soil As (Bednar et al., 2002; Datta et al., 2006). While the chief source of exposure is ingestion, secondary exposure occurs through inhalation and skin contact, particularly in occupational settings (Surdu et al., 2013).

The health hazard posed by soil As depends on several factors such as the mode and duration of exposure, type, the concentration of As, and its geochemical speciation. Mobility and bioavailability of soil As depend on its reactions with soil components and the stability of the solid-phase complexes (Rakhimbekova et al., 2021), which in turn depends on the physicochemical properties of the soil, such as pH, clay content, organic matter content, and the Fe/Al/Mn (hydr)oxides and sulfides that form relatively stable complexes with As making it less bioavailable (Datta et al., 2006). The bioavailability of soil As can be predicted by in-vitro bioaccessibility assays which are based on the solubility of As. However, it is necessary to validate the in-vitro bioaccessibility data using more realistic animal studies. Several studies have been undertaken to develop animal models such as swine and mice to generate realistic bioavailability values for As in soils (Bradham et al., 2020). An in-vitro model to predict the bioavailability of soil As was developed by Sarkar and Datta (2003) developed an in-vitro bioaccessibility model for soil As and validated the approach in-vivo (Makris et al., 2008). However, validating data from environmental samples using animal models is time and cost-prohibitive, in addition to posing ethical challenges. Furthermore, replicating the environmental conditions adds additional complexity to the experimental set-up and data analysis in in-vivo models.

Several studies have attempted to elucidate the transport and metabolism of toxic elements using in-vitro cell culture models (Meng and Meng, 2000; Dong, 2002; Martinez et al., 2011). Dong (2002) reported changes in signaling molecules (MAP kinases, p53, AP-1, and NF-κB) due to exposure to As using primary cultures of neonatal BALB/c epidermal cells. Zhao et al. (1997) reported DNA hypomethylation and aberrant gene expression using rat liver epithelial cell line and inoculation of nude mice, respectively. Meng and Meng (2000) reported blast transformation in human blood lymphocytes. Germolec et al. (1996) reported the overexpression of keratinocyte growth factors (granulocyte macrophage-colony stimulating factor and transforming growth factor-alpha) in human epidermal keratinocytes exposed to sodium arsenite. Since animal studies are expensive, require specialized facilities, and present ethical challenges, in-vitro chemical extraction methods have been employed to test the bioaccessibility of toxic elements. Cell culture models are relatively inexpensive, and easier to use when compared to in-vivo animal studies, and unlike bioaccessibility tests, can provide information on cellular toxicity. However, the studies reported in the literature have typically used various concentrations of commercially available As compounds as sources. Various in-vitro cell culture techniques have reported the toxicity of contaminated landfills and sewage sludge due to direct exposure (Jabłońska-Trypuć, 2021). However, a majority of the reported in-vitro cell studies use As salts at high concentrations that do not reflect the conditions of exposure to contaminated soils (Bradham et al., 2020). Specifically, the bioavailability of As salts in solution does not represent that in soil As. Thus, there is a lack of cell culture models to determine the effects of soil As that are environmentally relevant. While these studies have revealed several aspects of the impact of As on biological systems, they do not realistically represent environmental exposure from soils with varying physico-chemical properties. In this study, we developed a cell culture model to simulate exposure to soil As. Using a fractionation approach, we introduced various concentrations of As into cell cultures obtained from As-spiked Immokalee soil. Healthy Human Immortalized Keratinocyte (HaCaT) and Primary Human Dermal Fibroblasts (HDFa) cells were used. The HaCaT cells play a role in skin barrier homeostasis while the HDFa cells are fibroblast cells vital to cell proliferation and migration and participate in the interactions between epithelial and mesenchymal cells. Thus, changes in the responses of these cells on As exposure would represent the effect of soil As on vital cellular functions. Hence, these cell lines chosen serve as in-vitro models to assess contact exposure of As through the skin. The impact of the different environmentally relevant concentrations of soil As on cells was assessed through cell viability, scratch wound assay, immunocytochemistry, and western blotting.

2. Materials and methods

2.1. Soil incubation

Surface (0–15 cm) Immokalee series soil was collected from Southwest Florida Research and Education Center, Florida. Immokalee soil is a sandy spodosol, selected for this study due to its low As retention capability. The soil was dried at 100 °C and passed through a 2 mm sieve. The pH and electrical conductivity (EC) were measured. Four hundred grams of Immokalee soil were spiked with sodium arsenate (Na_2AsO_3) to achieve a final concentration of 45, 225, 450, and 900 mg of As per kg of soil. These concentrations were calculated based on the recommended arsenical pesticide application rates in agricultural fields in the U.S. in the early 20th century (Chisholm et al., 1955) and estimated As accumulation in soils resulting from 1, 3, 5, and 10 years of continuous arsenical pesticide application (Datta et al., 2006). Unspiked soil was considered as the control (C). The As-spiked soils were transferred to resealable storage bags and incubated in the greenhouse for six weeks. All the soils were maintained at 70% water-holding capacity. All samples were incubated in triplicate.

After six weeks, 1 g of soil (n = 3, N = 1) from each bag was acid-digested (USEPA 3050B) and analyzed for As using Perkin Elmer Optima 7000DV Inductively coupled plasma-optical emission spectrometry (ICP-OES) to obtain the

concentration of As. External commercial ICP metal standard solutions and an internal Yttrium standard were utilized to ensure the accuracy of the analysis. The concentrations of external standard solutions were set as 0, 0.01, 0.02, 0.05, 0.1, 0.2, 0.5, 1, 2, 5, 10, and 20 mg/L for each element. The internal Yttrium standard was set as 1 mg/L. The recovery of all standards was recorded at 95%–105%. The wavelengths used for Al, As, Cd, Co, Cr, Cu, Hg, Mn, Ni, Pb, and Zn in ICP-OES were 396.152, 188.980, 226.502, 238.892, 267.716, 324.754, 184.887, 257.610, 231.604, 220.353, and 213.857 nm, respectively. The Perkin Elmer Optima 7000DV ICP-OES was operated under the following parameters — Plasma gas flow: 15 L/min; Auxiliary gas flow: 0.5 L/min; Nebulizer gas flow: 0.80 L/min; RF power: 1400 W; Plasma view: axial; Read delay: 60 s; Sample pump flow rate: 1.5 mL/min; Spray chamber: Scott; Nebulizer: GemTip Cross-Flow II nebulizer; Injector: alumina; Quartz torch: single slot; replicates: 3

2.2. Sequential extraction

Geochemical fractionation of the soil (n = 3; N = 1) was performed using a sequential extraction method according Tessier et al. (1979) as modified by Sidhu et al. (2016). The following geochemical fractions of As in the Immokalee soils were extracted: water-soluble fraction (F-1), exchangeable fraction (F-2), carbonate-bound fraction (F-3), Fe- and Mn-bound fraction (F-4), organic-bound fraction (F-5), and residual-bound fraction (F-6). The extracts obtained after each step were centrifuged, 3500×g for 30 min, and analyzed for As using ICP-OES as mentioned in 2.1. The water-soluble fraction was used to treat the cells.

2.3. Cell culture

Normal Human Immortalized Keratinocyte cells (HaCaT) were obtained from Addexbio Technologies© (Catalog: T0020001). Primary Human Dermal Fibroblasts (HDFa) cells were obtained from American Type Cell Culture (PCS-201-012). The cells were maintained in modified Dulbecco's Modified Eagle's Medium (DMEM) (Thermofisher; Catalog: 128000). Media stock using tenfold concentrated powdered DMEM supplemented with 3.7 g/L of sodium bicarbonate was diluted with diH_2O and used to culture cells from passages 8–11 to acclimatize the cells. The media was supplemented with 10% Fetal Bovine Serum (FBS) (Gibco) and 1% Penicillin–Streptomycin (PS). The cells were cultured at 37 °C.

2.4. Extraction of water-soluble As from soil

The bioavailable fraction of As was extracted from the spiked soils using diH_2O in 1:15 (w/v) ratio. Three grams of each of the treatment and control soils were added to 45 ml of diH_2O in triplicates. The mixture was placed on an orbital shaker for 1 h at 250 rpm and then centrifuged at 3500 × g for 30 min. The supernatant was filtered, autoclaved, and analyzed for As using ICP-OES as mentioned in 2.1.

2.5. Soil As media preparation

3.5 ml of 10x DMEM media was added to 31.5 ml of water-soluble As fractions from each treatment and control. The final 1x media was filtered using 0.22 μm filters. 3.5 ml of FBS and 350 μl of Penicillin–streptomycin were added to the filtered media. 1 ml from each treatment and control replicate was diluted 10 times in diH_2 O and analyzed for As using ICP-OES to determine the final concentration of As in the treatment media. Cells grown in DMEM media (10% FBS, 1% PS) were considered as a negative control (NC).

2.6. Cell viability assay

The effect of different soil As concentrations on the viability of HaCaT and HDFa cells was determined using the CellTiter-Blue® Cell Viability Assay (Promega, Madison, WI). The calibrations and cell controls were determined according to the manufacturer's protocols. Briefly, the seeding density was determined for each cell line by performing cell titer blue optimization where 1000, 1500, 2000, 2500, and 3000 cells were seeded (n = 9, N = 1). After 24, 48, and 72 h the media was replaced with 180 μl media containing 30 μl of CellTiter-Blue® Cell Viability Assay reagent. Cell viability was measured after 2, 3, and 4 h of incubation at 37 °C. Analysis of variance (ANOVA, $p < 0.05$) was performed to determine the optimum seeding density and incubation period.

To evaluate the effect of soil As the cells were seeded in 48 well plates at an optimum seeding density of 2000 and 3000 cells per well for HaCaT and HDFa, respectively. The appropriate treatment and control media were added to the respective wells 24 h after cell seeding. After 24, 48 and, 72 h of treatment, the media was replaced with 180 μl media containing 36 μl of CellTiter-Blue® Cell Viability Assay reagent and placed in the incubator for 4 h. From this, 60 μl of the incubated medium was transferred to a 96-well clear-bottom, opaque-walled (black) culture plate (n = 12, N = 3). By measuring the fluorescent signal (Beckman Coulter DTX 880 Multimode Detector, ex/em at 560/590 nm) of the resorufin produced, cell viability was determined.

2.7. Scratch wound assay

Cell migration was quantitatively assessed using the scratch wound assay as reported by Liang et al. (2007). Cells (10,000 per well) were seeded in a 48-well plate. After the cells were confluent, 200 μl of respective treatment and control media, with n = 8, N = 3, were added. A scratch was made using a 200 μl pipette tip. Time-lapse images were captured every hour for 72 h using the EVOS FL Auto with an on-stage incubator. Wound closure due to cell migration were determined using Image J software (Schneider et al., 2012).

2.8. Cellular as uptake in the cells using Graphite Furnace Atomic Absorption Spectrometry (GFAAS)

Cells in exponential growing conditions in 6-well plates (n = 5, N = 3) were treated with media containing As prepared as explained in Section 2.5. After 72 h of treatment, the cells were washed with PBS, collected in 1.5 ml tubes using a cell scraper, and lysed using pre-cooled RIPA buffer and 1X protease inhibitor. Following lysis on ice for 20 min, the mixture was centrifuged at 12,000 rpm for 30 min. The pellet was discarded, and the supernatant was transferred to a fresh tube. The protein concentration of cell lysates (supernatant) was determined using the BCA Protein Assay kit (#23225, Thermo-Scientific, Waltham, MA, USA). Nitric acid (HNO_3; 750 μl) and Hydrogen Peroxide (H_2O_2; 250 μl) were added to the cells and digested under reflux conditions (135 °C) for 6 h in a dry bath block incubator (Hirano et al., 2013). Each resultant sample was analyzed for As using GFAAS. The resultant cellular As concentration was normalized to protein content (Hirano et al., 2013).

2.9. Immunocytochemistry

Qualitative expression of proteins was studied by immunocytochemistry. Cells (10,000) were seeded in 48 well plates and treated As-media (n = 6, N = 3). After 72 h, the cells were fixed with 4% paraformaldehyde (PFA) followed by three PBS washes of 10 minutes each. Fifty microliters of blocking buffer containing 1% Bovine serum albumin (BSA) were added, and the plate was placed on a shaker for 1 h. The cells were incubated with 50 μl of primary antibody on a shaker for 4 h at room temperature (RT) and then transferred to 4 °C overnight. Three replicates were prepared for each antibody tested anti-pan Akt (Rabbit, 1:1000; ab8805; abcam) and anti-CD44 (Mouse; 1:200; ab6124; abcam) and anti-pan Cad (Rabbit; 1:1000; ab1650; abcam) and anti-Zeb1 (Mouse; 1:500; ab181451; abcam). After washing with PBS, the secondary antibody, Goat Anti-Rabbit IgG H&L (Alexa Fluor® 488;1:1000; ab150077) was added to detect total Akt and total cadherin while sheep Anti-Mouse IgG H&L (Texas Red®; 1:1000; ab6806) was added to detect CD-44 and Zeb1. The secondary antibody treatments were done by incubating the cells in the dark at RT for 3 h. After PBS wash, the cells were stained with 50 μl of 300 nM DAPI (4′,6-Diamidino-2-Phenylindole, Dihydrochloride) (Invitrogen™; ThermoFisher Scientific D1306) at RT for 30 min. Following another PBS wash, fluorescent images were obtained using EVOS FL Auto.

2.10. Western blot

Western blot of HaCaT and HDFa cells after 72 h of soil As treatments were performed to observe cadherin and Akt expression. Cell lysates (n = 3, N = 3) were obtained according to recommended protocols as described in Section 2.8. The proteins were labeled with CF® dye 770 (Biotium, Catalog # 92222). Equal amounts of protein were loaded in the wells of a 10% pre-cast SDS-PAGE gel. Odyssey® 28 kDa Loading Indicator – 800 nm (LICOR, P/N: 926-20002) was added as a reference to each lane to evaluate the consistency of sample loading and uniformity of the western blot transfer. Chameleon duo pre-stained protein ladder® (LICOR, P/N: 928-60000) was added. Western blotting and antibody incubation was done according to recommended protocols. The primary antibodies, cadherin and Akt were the same as those used in immunocytochemistry. Donkey Anti-rabbit IR dye 680 RD (LICOR P/N: 926-68073) was used as the secondary antibody. Odyssey® Imaging system and Image Studio™ Lite quantification software were used for analysis.

2.11. In-cell western

Quantitative expression of Zeb1, CD44, and actin in HaCaT and HDFa were studied using In-cell western. The optimum seeding density was determined to be 3000 cells per well (96 well plate) for both HaCaT and HDFa cells (n = 9, N = 3). Cells were fixed with 3.7% PFA after 72 h of treatment. The cells were permeabilized in 0.1% Triton-X 100 in PBS. Intercept® (TBS) blocking buffer (LICOR P/N: 927-60001) was added to all the wells except the background wells (n = 3) and incubated for 3 h at RT. The primary antibodies CD44 and Zeb1 and beta-Actin antibody (Rabbit; 1:200; PA1-46296; Thermofisher) were diluted to recommended levels in TBS and added to the wells for overnight incubation at 4 °C. The cells were washed with 0.1% Tween-20 in PBS. Secondary antibodies IRDye® 800 CW Goat anti-Mouse IgG Secondary Antibody (1:500; LICOR; P/N: 926-32210) and IRDye® 800 CW Goat anti-Rabbit IgG Secondary Antibody (1:500; LICOR; P/N: 926-32211) were added to the background and treatment wells (n = 6) and incubated for 2.5 h at RT. CellTag™ 700 Stain for In-Cell Western™ Assays (1:500; LICOR; P/N: 926-41090) was added to three treatment wells. The plates were imaged and analyzed using the Odyssey® Imaging system and Empiria Studio®, respectively.

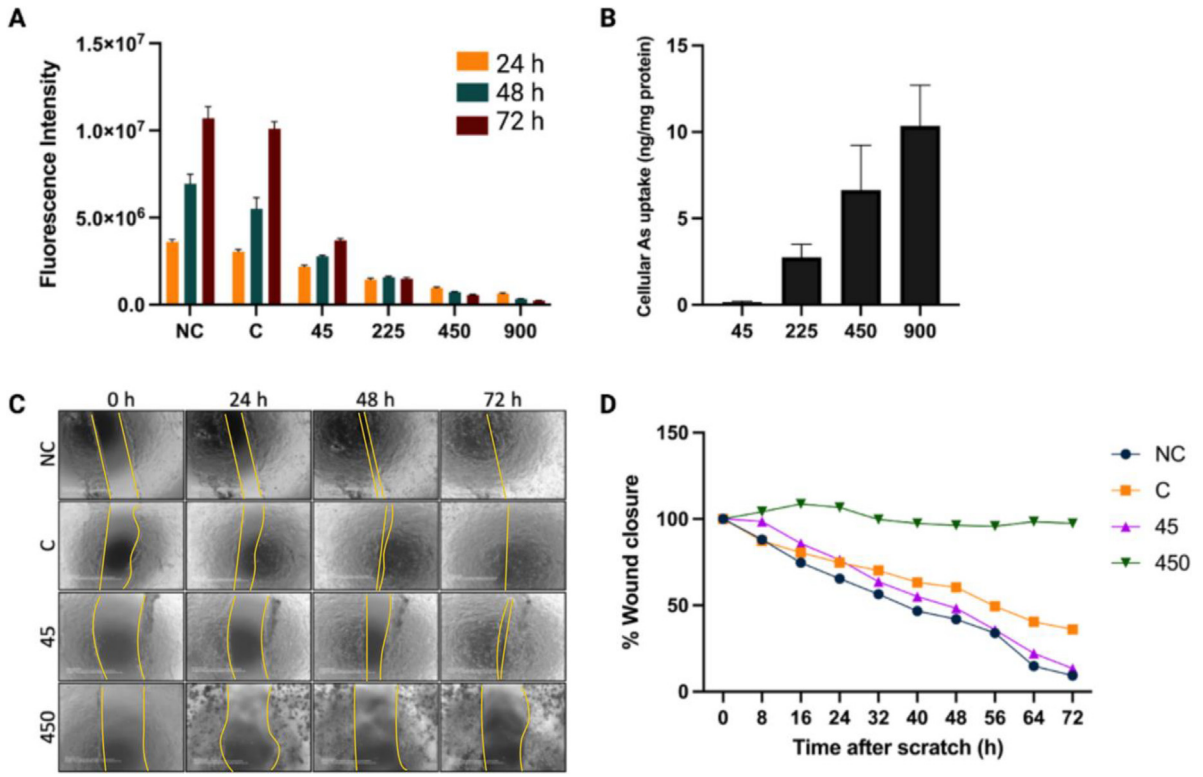

Fig. 1. Effect of soil As on HaCaT cell viability, cellular As uptake and cell migration. The cells were treated with four concentrations of soil As (45, 225, 450, and 900 mg/kg) and two controls — Negative control (NC — cells grown in media with no soil treatment) and control (C — cells treated with unspiked soil) for 72 h. HaCaT cell viability shows significant increase at 45 mg/kg soil and significant decrease at 450 mg/kg and 900 mg/kg soil As (1A). Cellular uptake of soil As by HaCaT cells increased with increasing soil As (1B). Scratch wound recovery of HaCaT cells (1C). Quantification of change in area of scratch using Image J (1D).

2.12. Statistical analysis

Student t-tests and Analysis of Variance (ANOVA) were performed using JMP® Pro 15 Statistical Software for CellTiter-Blue® Cell Viability Assay, cellular As uptake, Western blot, and In-cell western. The level of significance was set at p-value ≤ 0.05.

3. Results

3.1. Arsenic-media

The average pH and EC of the Immokalee soil samples were 5.44 $\pm$ 0.04 and 284.67 $\pm$25.11 μS/cm, respectively. The total As concentrations in the soil and media after extraction of the soluble fraction are shown in Table S1. Arsenic concentration in the media represents the soluble (bioavailable) fraction of As that can be easily absorbed by the skin cells. The amount of As in the media increased with increasing soil As concentrations.

3.2. Cellular As uptake

Cellular As uptake was estimated in HaCaT and HDFa cells exposed to the water-soluble fraction of As obtained from soils spiked with 45, 225, 450, and 900 mg/kg As. After 72 h of treatment, the amount of As taken up by both HaCaT and HDFa cells increased with increasing As concentrations. However, the uptake of As was significantly higher ($p < 0.001$) in HaCaT cells (Fig. 1B) compared to the HDFa cells (Fig. 2B).

3.3. Cytotoxicity of soil As on HaCaT and HDFa

The effect of soil As on HaCaT and HDFa cell viability was quantified using CellTiter-Blue® assay. In HaCaT cells, the cell viability decreased every 24 h with increasing concentrations of soil As but at lower As levels, a decreased rate of

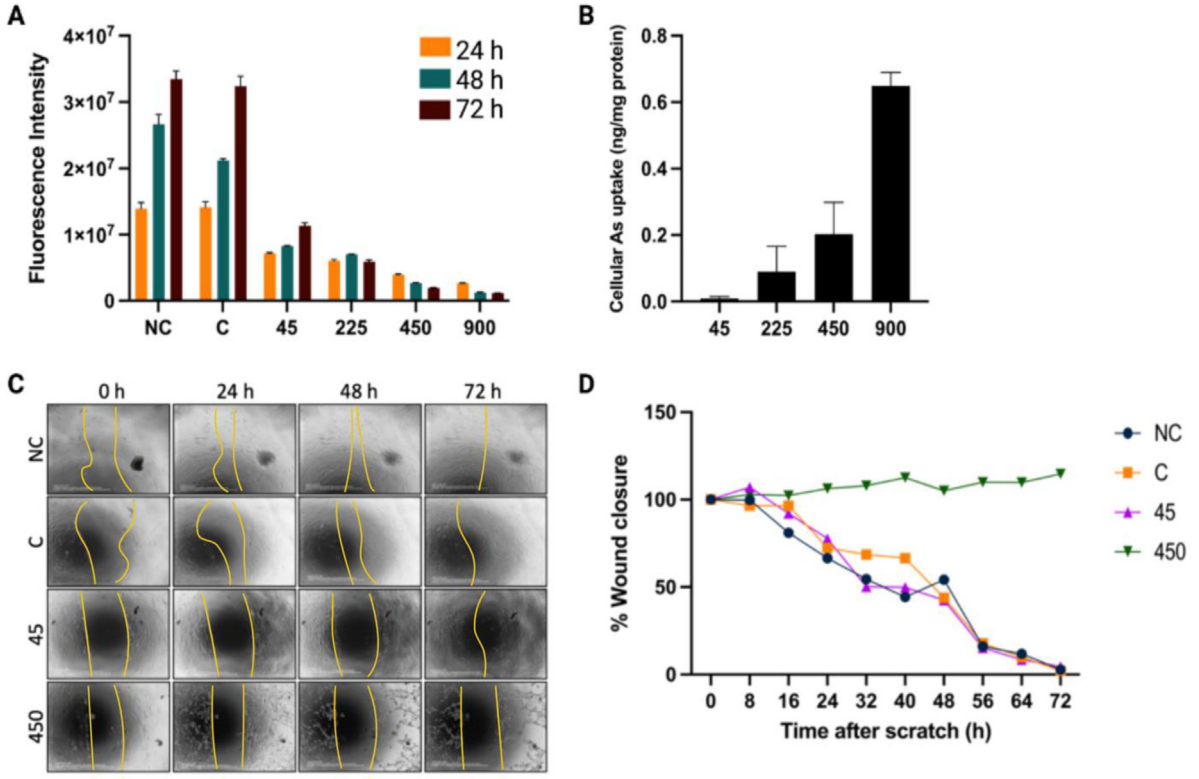

Fig. 2. Effect of soil As on HDFa cell viability, cellular As uptake and cell migration. The cells were treated with four concentrations of soil As (45, 225, 450, and 900 mg/kg) and two controls — Negative control (NC — cells grown in media with no soil treatment) and control (C — cells treated with unspiked soil) for 72 h. HDFa cell viability shows significant increase at 45 mg/kg soil and significant decrease at 450 mg/kg and 900 mg/kg soil As (1A). Cellular uptake of soil As by HaCaT cells increased with increasing soil As (1B). Scratch wound recovery of HDFa cells (1C). Quantification of change in area of scratch using Image J (1D).

proliferation was observed. A negative impact on cell viability in both HaCaT and HDFa cells was observed at higher As levels (450 and 900 mg/kg) of soil As (Figs. 1A and 2A).

In HaCaT cells, the cell viability in NC and C samples was significantly higher than the soil As treatments (45, 225, 450, and 900 mg/kg) after 24 h of treatment. There was no significant difference between NC and C samples. After 48 h, the cell viability in NC, C, and 45 mg/kg increased significantly ($p < 0.001$). Cell viability in 225 mg/kg increased at 48 h, but it was not significant. At higher soil As treatments (450 and 900 mg/kg) there was a significant decrease in cell viability. After 72 h, the cell viability in NC, C, and 45 mg/kg increased significantly. There was a non-significant decrease in the cell viability in the 225 mg/kg treatments after 72 h compared to 48 h, but decreased significantly in 225, 450, and 900 mg/kg (Fig. 1A).

In HDFa cells, the cell viability in NC and C samples was significantly higher than the soil As treatments (45, 225, 450, and 900 mg/kg) after 24 h of treatment. After 48 h, there was a significant increase in cell viability in NC, C, 45, and 225 mg/kg. The cell viability in NC and C samples showed no significant difference. At higher concentrations of 450 and 900, the cell viability decreased significantly. After 72 h, the cell viability in NC, C, and 45 mg/kg increased. There was a significant ($p < 0.0001$) decrease in the cell viability at 225, 450, and 900 mg/kg (Fig. 2A).

Overall, there was no significant difference in cell viability at 225 mg/kg over 72 h in HaCaT and HDFa cells. The cell viability increased significantly in NC, C, and 45 but decreased significantly at 450 and 900 mg/kg after 72 h.

3.4. Scratch wound assay

The effect of soil As on wound healing of dermal cells (HaCaT and HDFa) was determined using the scratch wound assay. Wound healing was recorded for a 72-h duration when the wound closure or percentage change in the area of the scratch was evaluated in treated and control dermal cells.

In HaCaT cells, 20% of the scratch was repaired in NC and C after 24 h. With increasing concentration of soil As, the wound repair slowed down. At 45 mg/kg, there was 18% wound closure, indicating very little impact on wound healing at a lower level of As. However, at higher concentrations, the scratch failed to heal (Figs. 1C, 1D; S1). After 48 h, the migrating HaCaT cells repaired almost 60% of the scratch in NC and C. In the 45 mg/kg treatment, about 50% of the scratch was

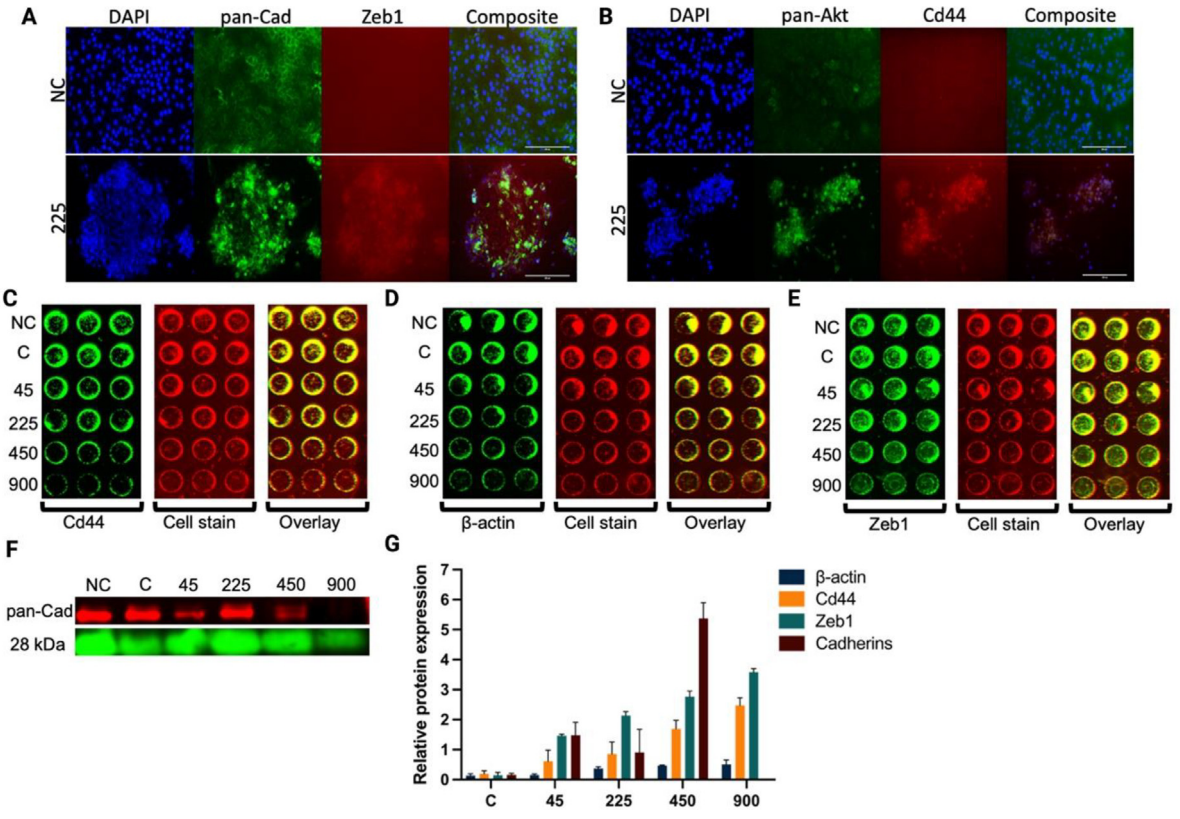

Fig. 3. Expression and quantification of Cadherin, Zeb1, Akt, and CD44 in HaCaT cells. The cells were treated with four concentrations of soil As (45, 225, 450, and 900 mg/kg) and two controls — Negative control (NC – cells grown in media with no soil treatment) and control (C – cells treated with unspiked soil) for 72 h. Qualitative expression of Cadherin and Zeb1 (3A) and CD44 and Akt (3B) were determined using immunocytochemistry. Quantitative expressions of CD44 (3C), β-Actin (3D), Zeb1 (3E), and Cadherin (3F). The $\log_2$ fold change is representative of the change in expression of the protein with respect to the negative control in each case ($p < 0.05$) (3G).

repaired, but at 225, 450, and 900 mg/kg treatments, there was a decrease in the covered area indicating a lack of repair after 48 h (Figs. 1C, 1D; S1). This could be attributed to the negative impact of soil As on cell proliferation and migration. After 72 h, 90% wound closure was observed in NC, C, and 45 mg/kg. This indicates that cell migration of HaCaT cells was not affected due to the presence of low levels of As. There was no overall change in scratch in treatments 225, 450, and 900 mg/kg after 72 h indicating the toxic effect of soil As on cell proliferation and migration (Figs. 1C, 1D; S1)

In HDFa cells, 24 h after the scratch, there was 20% wound closure in NC, C, and the 45 mg/kg treatments. There was a 3.5% recovery in the area of scratch in 45 mg/kg. There was an increase in area of scratch for the 450 and 900 mg/kg treatments (Figs. 2C, 2D; S2) due to the impact of higher concentrations of As on cell migration. After 48 h, there was 58% wound closure in NC and C. Similarly, there was 58% and 23% wound closure in 45 and 225 mg/kg respectively. At higher concentrations of As, there was an increase in the area of the scratch. After 72 h, there was 97% wound closure in NC, C, and 45 mg/kg treatments. There was a steady increase in cell migration in 225 mg/kg after 40 h and there was 56% closure of the wound after 72 h. However, there was no decrease in the area of scratch in 450 and 900 mg/kg treatments. Overall, cell migration was not affected in the 45 treatment, and wound healing followed a similar trend as NC and C (Fig. S3). In 225 mg/kg, the cell migration rate was lower compared to NC, C, and 45 mg/kg. At 450 and 900 mg/kg there was an increase in the area of the scratch. This could be attributed to a reduction in cell proliferation and the cytotoxicity of As (Figs. 2C, 2D, S2).

3.5. Cell adhesion and migration proteins impacted by soil arsenic

Expression of Cadherins and Zeb1 were observed using Immunocytochemistry, Western Blot (WB) and In-cell Western (ICW) assays. Immunocytochemistry of HaCaT (Fig. 3A) and HDFa (Fig. 4A) cells showed a change in the expression levels of Cadherin (total) and Zeb1 in both HaCaT and HDFa cells.

In HaCaT cells Zeb1 expression was observed for 225, 450, and 900 mg/kg As treatments. There was an increase in the expression of Cadherins at 225 mg/kg (Fig. 3A). Expression of Cadherins in 450 and 900 mg/kg treatments decreased compared to those of NC, C, and 45 mg/kg (Fig. S4). However, the number of viable cells was low at higher As

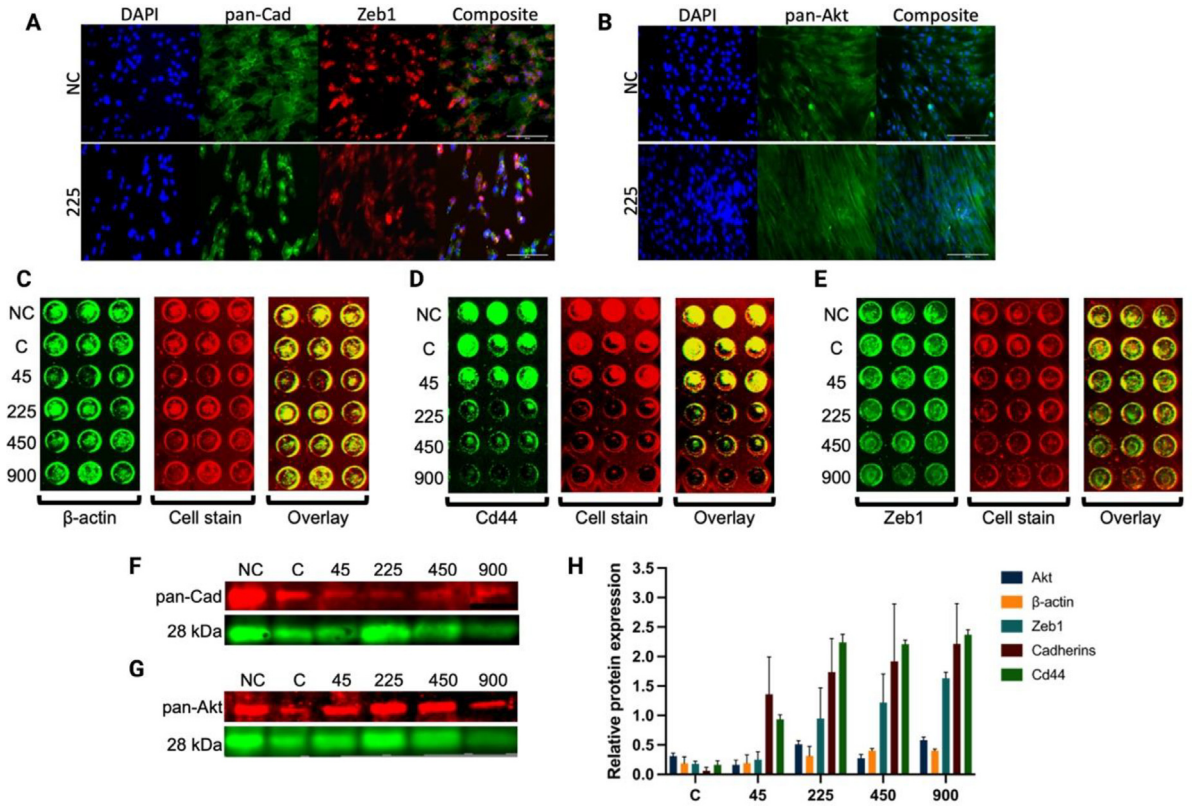

Fig. 4. Expression and quantification of Cadherin, Zeb1, Akt, and CD44 in HDFa cells. The cells were treated with four concentrations of soil As (45, 225, 450, and 900 mg/kg) and two controls — Negative control (NC — cells grown in media with no soil treatment) and control (C — cells treated with unspiked soil) for 72 h. Qualitative expression of Cadherin and Zeb1 (3A) and Akt (3B) were determined using immunocytochemistry. Quantitative expressions of β-Actin (4C), CD44 (4D), Zeb1 (4E), Cadherin (4F), and Akt (4G). The $\log_2$ fold change is representative of the change in expression of the protein with respect to the negative control in each case ($p < 0.05$) (4H).

concentrations. In NC, C, and 45 mg/kg treatments, Cadherins were expressed at the cell membranes (Fig. S4). However, at 225, 450, and 900 mg/kg the expression was within the cells. The quantified expression of Zeb1 (Fig. 3E) and Cadherin (3F) data show a significant change in the treatments compared to the control. There was no Cadherin detected for the 900 mg/kg treatment in HaCaT cells (Fig. 3F).

In HDFa cells, Zeb1 expression decreased at 225 mg/kg, and there was a change in the expression of Cadherin at higher concentrations of As (Fig. 4A). These results were quantified using WB for Cadherin (Fig. 4F) and ICW for Zeb1 (Fig. 4E). Figs. 3G and 4H show that cadherin expression changed with increasing concentrations of soil As in HDFa cells. There was no significant difference in expression until the 225 mg/kg treatment. But there was a significant increase in Cadherin expression at the 450 mg/kg treatment. Fig. 4E shows a progressive increase in Zeb1 expression with an increase in soil As concentration.

3.6. Expression of Akt, CD44, and β-actin

Immunocytochemistry showed a change in Akt expression with increasing soil As concentration until 225 mg/kg as shown in Figs. 3B and S5 in HaCaT cells. In HDFa cells there were no changes observed in the levels of Akt expression (Figs. 4G and S6) at 225 mg/kg soil As. Quantification of Akt expression using WB also showed no significant difference in the expression of both HaCaT and HDFa (Figs. 3G and 4H).

Immunocytochemistry of HaCaT cells after 72 h of As treatment showed the expression of CD44 at 225, 450, and 900 mg/kg (Figs. 3B and S4). There was no CD44 expression observed in HDFa cells after immunostaining. Quantitative data obtained from ICW indicated that HaCaT cells had a gradual increase in CD44 expression with increasing As concentration (Figs. 3C, 3G, and S7-A). In HDFa cells, CD44 expression remained constant in NC, C, and 45 mg/kg (Figs. 4D, 4H, and S7-D). However, the signal detected was very low when treated with higher As concentrations. Figs. 3D and 3G show an increase in β-actin expression after 72 h of As treatment on HaCaT cells. The expression levels of β-actin in HDFa were similar at all concentrations (C, 45, 225, 450, and 900 mg/kg) of As with a fold change of less than 0.5 (Figs. 4C and 4H).

4. Discussion

Arsenic is a group 1 human carcinogen, and exposure to As through various routes, including ingestion, inhalation, and dermal contact is a growing concern. One of the major environmental causes of As-related cancer worldwide is due to the use of As-contaminated groundwater for drinking and irrigation purposes (Duong et al., 2021). High As concentration in groundwater results from the dissolution of As-containing rocks and minerals. Arsenic accumulation also occurs through various anthropogenic activities such as the use of As pesticides, wood preservatives, mining activities, and the disposal of industrial waste and sewage materials (Datta et al., 2006). Long-term use of phosphate fertilizer combined with As-based pesticides has increased the mobile inorganic As in the soil (Hartley et al., 2013). Previous studies have shown that As exposure to contaminated dust, water, and leachates can lead to skin diseases due to direct dermal exposure (Alimba et al., 2016; Bradham et al., 2020; Palma-Lara et al., 2020). Health risk characterization using dermal bioaccessibility models showed a high risk of toxic element exposure from contaminated soil and mine tailing due to direct skin contact (Leal et al., 2018). Huang et al. (2015) reported that keratinocytes were more sensitive to dust and metal (oid) contaminants in the water-soluble fraction. Arsenical pesticides are the major reason for soil As contamination in agricultural fields all over the world (Bencko and Li Foong, 2017). Rahman et al. (2019) reported soil As concentrations up to 4500 mg/kg in cattle dipping sites in northern Australia. Apple orchard farms in the Northeastern states of the U.S. have up to 50 mg/kg soil As (Shavit and Shavit, 2010). High concentrations of soil As have also been found in wetlands of China (67 mg/kg) and horticulture farms in Australia (100 mg/kg) due to the extensive use of arsenical pesticides (Lin et al., 2015; Chen et al., 2021; Conrad et al., 2021). Datta et al. (2006) calculated the As accumulation in the soil after 1-, 3-, 5-, and 10 years of continuous use of arsenical pesticides to be 45, 225, 450, and 900 mg/kg respectively. In this study, we chose four soil As concentrations based on 10 year use of arsenical pesticides as a representation of accumulation of As in soil due to years of pesticide use, to develop the in-vitro cell culture model.

The bioavailability of As in the human body is a major factor in determining the toxicity of soil As. Bioavailability of soil As depends upon soil properties such as pH, particle size, clay content, organic matter content, and the presence of oxides of iron, manganese and aluminum (Quazi et al., 2010). In addition, the bioavailability of soil As depends on weathering, chemical aging of the soil, as well as microbial processes (Bradham et al., 2015). The toxic effect of As-contaminated soil is a complex phenomenon that is difficult to measure. Previous studies have reported Biological testing to measure the bioavailability and the toxic impact of soil As are performed using in-vivo tests using mammals, such as mouse, rabbit or juvenile swine models (Henry et al., 2015). For example, studies have reported the accumulation of As in toenails, blood, hair, and urine in animal models by performing As bioavailability studies using contaminated soils (Li et al., 2017; Bradham et al., 2020). Agricultural soil samples with up to 4495 mg/kg of soil As have been tested using in-vivo methods (Bradham et al., 2018; Bagherifam et al., 2019). However, these tests are expensive, require specialized facilities, and are ethically challenging. Hence, human cell lines are increasingly being used as in-vitro systems to understand the toxicological effects of environmental contaminants.

In this study, we investigated the effects of As on skin cells caused by direct dermal exposure to soil spiked with As using HaCaT and HDFa cell lines. To our knowledge, there is a lack of detailed evaluation of the cytotoxic effects of soil As on skin cells. To successfully study the effect of soil As exposure on skin cells, we extracted the bioavailable fraction of As from the soil as opposed to using commercially available As salts (Xue et al., 2017). The goal of this study was to develop an in-vitro cell culture model that can be used to test the cytotoxic and proteomic effects of soil As on skin cells due to direct dermal exposure.

Immokalee soil used for this study has a low As retention capacity. We observed that most of the As were found in the water-soluble fraction, as was previously reported by Quazi et al. (2010). The water-soluble As is expected to be easily absorbed by the skin cells during direct dermal exposure (Jabłońska-Trypuć, 2021). We observed that cytotoxicity of HaCaT and HDFa cells was affected by soil As. Specifically, with increasing soil As there was a decrease in the average cell viability at each time point tested. This data fits with the report by Udensi et al. (2011) that indicated that sodium arsenate was cytotoxic to HaCaT cells, and the cell viability decreased with increasing As concentration. At 45 mg/kg soil As treatment in our study, the cell viability increased with time. This indicates that soil As does not affect cell proliferation at lower concentrations, but with increasing concentrations, As impacts cell proliferation in both HaCaT and HDFa cells (Figs. 1A and 2A). It is important to note that previous reports for skin fibroblast cells exposed to As used 100 μM concentration for As (Baumgartner et al., 2004; Chayapong et al., 2017). In our studies, we used up to 32 mM (Chayapong et al., 2017) to reflect the As content available in environmental soil samples.

To further support our findings on the cytotoxic effect of soil As on cells, we performed scratch wound assay on HaCaT and HDFa cells. Scratch wound assays are an excellent in-vitro method to study the effect of various treatments on cell migration, embryonic development, wound healing, as well as tissue inflammation, and cancer progression (Mia and Singh, 2019; Pijuan et al., 2019). This assay has been used in testing various drugs. Recently, researchers developing biomaterials for wound dressing that incorporates nanoparticles have used scratch wound assays to test their wound healing properties (Ismail et al., 2019). In this study, our objective was to track the effect of As on cell migration and wound healing. Previously, Walter et al. (2010) reported that the rate of fibroblast recovery was higher than keratinocytes. This behavior was also seen in the presence of soil As. The HDFa cells in NC, C, 45 and 225 mg/kg were able to heal the scratch compared to HaCaT cells that healed the scratch only in NC, C, and 45 mg/kg. This indicates that while soil As impacts the migration rate in fibroblasts, the cells remain viable even at 225 mg/kg soil As. However, the keratinocytes appear to be more susceptible to soil As (Figs. 1C, 1D, 2C, and 2D) at all concentrations.

Epithelial–Mesenchymal Transition (EMT) is associated with physiological response to wounds or stress on cells. The epithelial cells transform to gain mesenchymal characteristics during tissue regeneration or cancer progression (Ribatti et al., 2020). In addition, for the cells to migrate, changes in adhesion markers are anticipated. Cadherins are transmembrane proteins that mediate cell-to-cell adhesion. They are responsible for cellular migration and help maintain the cytoskeletal structure of the cell (Jiang et al., 2013; Rajwar et al., 2015). Zinc finger E-box binding homeobox 1 or ZEB1 is a known EMT activator (Sánchez-Tilló et al., 2011; Zhang et al., 2015; Chiu et al., 2017). Dermal fibroblasts have been reported to express ZEB1 and regulate the expression of cadherins, specifically E-cadherin (Denecker et al., 2014; Konradi et al., 2014; Yi et al., 2018; Singh et al., 2019). In the event of an injury, the epithelial cells and macrophages express ZEB1, regulate the expression of cadherins, and affect cell migration and healing, while the overexpression is linked to loss of regulation of E-cadherin and metastasis. Similarly, mutation of the ZEB1 gene has been reported to affect E-cadherin and loss of expression of vimentin leading to alterations in cell adhesion and migration. Zeb1 is often correlated with the expression of Cadherin. Although the actual function of Zeb1 is not completely understood, it is associated with cellular plasticity. The expression of Zeb1 is connected to cellular transformation due to changes in environmental conditions or stress (Llorens et al., 2019; Drápela et al., 2020). Weinmuellner et al. (2018) reported that the presence of chronic low-level As altered the expression of cadherin and Zeb1 in HaCaT cells. Similar results were observed in our study using HaCaT cells (Fig. 3). The change in Cadherin expression indicated a shift in cell-to-cell adhesion and migration. The higher fold change with increasing soil As implies the Cadherin levels are affected. The Zeb1 expression decreased with increasing concentrations of soil As treatments. Cadherin and Zeb1 expression in HaCaT cells can be linked to cell viability and cell migration data. The cell viability and wound healing were not adversely affected in the presence of low concentrations of soil As; the fold change in levels of Cadherins was not significant at 45 and 225 mg/kg (Fig. 3G). This indicates that low concentrations of soil As do not transform the HaCaT cells however, at higher concentrations of soil As possible cellular transformation affects the levels of EMT proteins.

The EMT protein expression was also affected in HDFa cells. Arsenic-mediated expression of N-cadherin and vimentin has been reported by Thang et al. (2014). However, healthy HDFa cells also express Zeb1 and can be affected due to external stress (Yi et al., 2018). In the presence of soil As Zeb1 was downregulated, and cadherin levels also decreased, indicating cellular transformation by affecting Zeb1 and N-cadherin. In HDFa cells, soil As downregulated the expression of Zeb1 when compared to NC.

To further explore the potential cellular transformation of HaCaT and HDFa cells by soil As, we observed Akt and CD44 levels. Akt, also known as protein kinase B (PKB) is a cell growth promoter. The phosphatidylinositol 3-kinase (PI3K)/protein kinase B (Akt) signaling pathway plays a key role in cell proliferation, differentiation, migration, metabolism, and angiogenesis thereby affecting wound healing. Furthermore, PI3K/Akt has been implicated in cancers of the skin with poor outcomes. Overexpression of Akt is linked to cell transformation, increase in cell proliferation, and metastatic features (Teng et al., 2021). Akt plays an essential role in various cell signaling pathways like PI3K/Akt/mTOR, JNK/Akt/STAT3 (Wang et al., 2012). A change in the levels of Akt can affect various downstream proteins that control and maintain cell stability. Arsenic-induced overexpression of Akt is linked to an increase in the migration of As-induced transformed cells in skin, bronchial, and prostate epithelial cells (Wang et al., 2012; Jiang et al., 2013; Ngalame et al., 2014; Teng et al., 2021). According to immunocytochemistry data, the Akt levels in HaCaT cells were affected by soil As. Akt was expressed in NC, C, and 45 soil As treatments at the membranes. However, at 225, 450, and 900, Akt is expressed inside the cell. Although we could not observe an overexpression of Akt in HaCaT cells, the change in expression indicates that Akt levels were affected in the presence of soil As. Previous studies have reported that As-induced change in Akt levels is associated with cell transformation (Wang et al., 2012; Chen et al., 2019). Overall, there was no significant change in the Akt levels of HDFa. This can be correlated to the cell migration data, that cells could heal the scratch wound in 225 mg/kg soil As treatment.

CD44 is a glycoprotein that is responsible for hematopoiesis and maintaining extracellular interactions. It also plays an important role in EMT regulation through its role in cell proliferation, migration, and apoptosis. CD44 is overexpressed in malignant melanoma and contributes to poor prognosis (Dietrich et al., 1997; Senbanjo and Chellaiah, 2017). Overexpression of CD44 can promote the expression of EMT by activating Akt signaling pathways (Mesrati et al., 2021; Primeaux et al., 2022). Previous studies report that As induces EMT transformation and alters the CD44 levels (Zhou et al., 2021; Yang et al., 2022). The CD44 expression in HaCaT supports these conclusions. CD44 expression was observed at 225 mg/kg according to our immunocytochemistry data. As mentioned earlier, there was a change in the expression of Akt and Zeb1 at 225 mg/kg. This indicates that at 225 mg/kg soil As, HaCaT cells undergo transformation altering the EMT transformation and thus changing the CD44 levels. The overall expression of CD44 expression was low and not detected using immunocytochemistry. However, CD44 expression using ICW shows that there was a significant change in CD44 expression at 45 compared to NC and C, but there was no significant change observed between 225, 450, and 900 mg/kg (Figs. 3C and 3G). In HDFa cells, there was no significant change in Akt and EMT protein expression data. However, was a significant difference in CD44 expression with increasing soil As (Figs. 4D and 4H). This indicated that HDFa cells did not undergo transformation, however, were susceptible to soil As toxicity according to cell viability and cell migration data.

The main function of β-actin is to maintain cell stability and promote cell migration and proliferation. β-actin is a housekeeping gene that is used as a control for protein expression studies because it is expressed in abundance in eukaryotic cells, and their expression levels are generally not altered due to various treatments (Bunnell et al., 2011). However, recent studies have reported that β-actin is not a reliable housekeeping gene as β-actin levels are affected

due to treatments targeting the cytoskeletal structure of the cell (Ruan and Lai, 2007). Thus, we used Odessey® 28 kDa loading indicator to normalize the western blot. Loading indicators allow consistent sample loading and uniform western blot transfer (Aldridge et al., 2008; Thacker et al., 2016; Butler et al., 2019; Pillai-Kastoori et al., 2020). Previous studies indicate that As can affect the cytoskeletal structure of the cells and alter the actin expression (Sanyal et al., 2020; Lin et al., 2021). Our data show that soil As affects the cytoskeletal structure of HaCaT cells, which could induce cellular transformation. The effect on the cytoskeletal structure could also promote the change in Akt expression as observed from the IHC experiments. However, in the case of HDFa cells, the β-actin levels were not altered, indicating that soil As does not affect the cytoskeletal structure of dermal fibroblasts.

Finally, the cellular As uptake data reflects the total As uptake in the cells. Previous studies have shown that with an increase in As, the cellular uptake of As increases (Hirano et al., 2013; Liu et al., 2019). Our data showed similar trends, the cellular As uptake increased with an increase in soil As concentration. However, the concentration of As in HDFa cells was much lower than HaCaT cells. This indicates that HDFa cells do not take up much As even in the presence of high soil As, although the cell viability data clearly showed that soil As is cytotoxic.

Collectively these findings suggest that exposure to soil As is toxic to the cells. HaCaT cells are more susceptible to As-induced cellular transformation compared to HDFa. The 450 and 900 mg/kg soil As treatments had exponentially higher As concentrations compared to the controls and lower soil-As treatments (45 and 225 mg/kg) (Table S1). While the data indicated high toxicity, 450 and 900 mg/kg did not yield conclusive results related to soil As-induced cell transformation. The 45 and 225 mg/kg soil As treatments can be further explored to understand the As-mediated cellular transformation. Furthermore, our work here indicates that In-cell western is a more sensitive and higher throughput technique to quantify protein expression and detect low signals of protein expression, compared to western blot which involves lysing of the cells and detecting proteins based on size. The approach presented here demonstrates the efficacy of ICW and is the first reported demonstration of cellular toxicity of soil As using this technique.

We were able to develop a working model to test soil As on skin cells by simulating realistic environmental exposure conditions for dermal contact. The fractionation model can be extended to study the effect of soil As and other metal and non-metal contaminants on human health caused by exposure through dermal contact using soil samples with varying soil physico-chemical properties. In-vivo systems are not reliable and often do not replicate the results of clinical studies (Van Norman, 2019). Alternatively, the in-vitro model developed in this study can be used as a quick, inexpensive, and reliable approach to determine the toxicity of soil contaminants. So far, most studies with in-vitro models have focused on the toxicity of drugs. However, recently there is increased interest in developing clinically relevant in-vitro models to replicate environmental exposure using cell culture (Truskey, 2018). Only a few studies have examined the effect of soil pollutants on human cell lines using in-vitro cell culture systems. The in-vitro protocol developed in this study has the potential to serve as a model to test the effects of various environmental soil pollutants through dermal exposure. Future studies on developing cellular models for exposure to soil As through ingestion and inhalation using the principle of extraction of bioavailable As are in progress. Developing these cellular models will significantly improve the current state of scientific knowledge that is expected to result in the generation of more reliable risk numbers from As-exposure assessments.

Funding

Great Lakes Research Center (GLRC) – GLRC Student Research Grant Award, Michigan Technological University; Dr. and Mrs. Songer (Songer Research Award).

CRediT authorship contribution statement

Manas Warke: Methodology, Investigation, Conceptualization, Writing – original draft. **Madeline English:** Methodology. **Laura De Marchi:** Methodology, Visualization. **Rohan Deep Sarkar:** Methodology, Visualization. **Srinivas Kannan:** Methodology. **Rupali Datta:** Investigation, Conceptualization, Writing – review & editing. **Smitha Rao:** Investigation, Conceptualization, Writing – original draft, Writing – review & editing.

Declaration of competing interest

The authors declare that they have no known competing financial interests or personal relationships that could have appeared to influence the work reported in this paper.

Data availability

The datasets generated during the current study are available in the Digital Commons repository, "Using Scratch Wound Assay To Study The Effect of Soil Arsenic on keratinocytes" by Manas Warke, Laura De Marchi et al. and "Using Scratch Wound Assay To Study The Effect of Soil Arsenic on fibroblasts" by Manas Warke, Laura De Marchi et al.

Acknowledgments

The authors would like to acknowledge the financial support for Manas Warke and Srinivas Kannan from Health Research Institute (HRI), Great Lakes Research Center, and Department of Biological Sciences at Michigan Technological University, United States. Dr. Zhiming Zhang from Stevens Institute of Technology is acknowledged for samples analysis using GFAAS.

Appendix A. Supplementary data

Supplementary material related to this article can be found online at https://doi.org/10.1016/j.eti.2022.102949.

References

Aldridge, G.M., Podrebarac, D.M., Greenough, W.T., Weiler, I.J., 2008. The use of total protein stains as loading controls: An alternative to high-abundance single-protein controls in semi-quantitative immunoblotting. J. Neurosci. Methods 172, 250–254.

Alimba, C.G., Gandhi, D., Sivanesan, S., Bhanarkar, M.D., Naoghare, P.K., Bakare, A.A., Krishnamurthi, K., 2016. Chemical characterization of simulated landfill soil leachates from Nigeria and India and their cytotoxicity and DNA damage inductions on three human cell lines. Chemosphere 164, 469–479.

Bagherifam, S., Brown, T.C., Fellows, C.M., Naidu, R., 2019. Bioavailability of arsenic and antimony in terrestrial ecosystems: A review. Pedosphere 29, 681–720.

Baumgartner, M., Sturlan, E., Wessner, B., Bachleitner-Hofmann, T., 2004. Enhancement of arsenic trioxide-mediated apoptosis using docosahexaenoic acid in arsenic trioxide-resistant solid tumor cells. Int. J. Cancer 112, 707–712.

Bednar, A.J., Garbarino, J.R., Ranville, J.F., Wildeman, T.R., 2002. Preserving the distribution of inorganic arsenic species in groundwater and acid mine drainage samples. Environ. Sci. Technol. 36, 2213–2218.

Bencko, V., Li Foong, F.Y., 2017. The history of arsenical pesticides and health risks related to the use of agent blue. Ann. Agric. Environ. Med. 24, 312–316.

Benipal, G., Harris, A., Srirajayatsayai, C., Tate, A., Topalidis, V., Eswani, Z., Qureshi, M., Hardaway, C.J., Galiotos, J., Douvris, C., 2017. Examination of Al, As, Cd, Cr, Cu, Fe, Mg, Mn, Ni, Pb, Sb, Se, V, and Zn in sediments collected around the downtown Houston, Texas area, using inductively coupled plasma-optical emission spectroscopy. Microchem. J. 130, 255–262.

Bradham, K., Diamond, G., Juhasz, A., Nelson, C., Thomas, D., 2018. Comparison of mouse and swine bioassays for determination of soil arsenic relative bioavailability. Appl. Geochem. 88, 221–225.

Bradham, K., Herde, C., Herde, P., Juhasz, A.L., Herbin-Davis, K., Elek, B., Farthing, A., Diamond, G.L., Thomas, D.J., 2020. Intra-and interlaboratory evaluation of an assay of soil arsenic relative bioavailability in mice. J. Agricult. Food Chem. 68, 2615–2622.

Bradham, K.D., Nelson, C., Juhasz, A.L., Smith, E., Scheckel, K., Obenour, D.R., Miller, B.W., Thomas, D.J., 2015. Independent data validation of an in vitro method for the prediction of the relative bioavailability of arsenic in contaminated soils. Environ. Sci. Technol. 49, 6312–6318.

Bunnell, T.M., Burbach, B.J., Shimizu, Y., Ervasti, J.M., 2011. β-actin specifically controls cell growth, migration, and the G-actin pool. Mol. Biol. Cell 22, 4047–4058.

Butler, T., Jonathan, A.J., Paul, W., Chan, E.-C., Smith, R., Tolosa, J.M., 2019. Misleading westerns: Common quantification mistakes in western blot densitometry and proposed corrective measures. Biomed Res. Internatl. 5214821. http://dx.doi.org/10.1155/2019/5214821, PMID: 30800670; PMCID: PMC6360618.

Chayapong, J., Madhyastha, H., Madhyastha, R., Nurrahmah, Q.I., Nakajima, Y., Choijookhuu, N., Hishikawa, Y., Maruyama, M., 2017. Arsenic trioxide induces ROS activity and DNA damage, leading to G0/G1 extension in skin fibroblasts through the ATM-ATR-associated chk pathway. Environ. Sci. Pollut. Res. 24, 5316–5325.

Chen, Y., Liu, X., Wang, H., Liu, S., Hu, N., Li, X., 2019. Akt regulated phosphorylation of GSK-3β/cyclin D1, p21 and p27 contributes to cell proliferation through cell cycle progression from G1 to S/G2M phase in low-dose arsenite exposed HaCat cells. Front. Pharmacol. 1176.

Chen, W., Zhu, K., Cai, Y., Wang, Y., Liu, Y., 2021. Distribution and ecological risk assessment of arsenic and some trace elements in soil of different land use types, Tianba Town, China. Environ. Technol. Innov. 24, 102041.

Chisholm, D., MacPhee, A.W., MacEachern, C.R., 1955. Effects of repeated applications of pesticides to soil. Can. J. Agric. Sci. 35 (5), 433–439.

Chiu, L.Y., Hsin, I.L., Yang, T.Y., Sung, W.W., Chi, J.Y., Chang, J.T., Ko, J.L., Sheu, G.T., 2017. The ERK–ZEB1 pathway mediates epithelial–mesenchymal transition in pemetrexed resistant lung cancer cells with suppression by vinca alkaloids. Oncogene 36, 242–253.

Conrad, S.R., White, S.R., Santos, I.R., Sanders, C.J., 2021. Assessing pesticide, trace metal, and arsenic contamination in soils and dam sediments in a rapidly expanding horticultural area in Australia. Environ. Geochem. Health 43, 3189–3211.

Datta, R., Sarkar, D., Sharma, S., Sand, K., 2006. Arsenic biogeochemistry and human health risk assessment in organo-arsenical pesticide-applied acidic and alkaline soils: An incubation study. Sci. Total Environ. 372, 39–48.

Denecker, G., Vandamme, N., Akay, Ö., Koludrovic, D., Taminau, J., Lemeire, K., Gheldof, A., De Craene, B., Van Gele, M., Brochez, L., 2014. Identification of a ZEB2–MITF–ZEB1 transcriptional network that controls melanogenesis and melanoma progression. Cell Death Differ. 21, 1250–1261.

Dietrich, A., Tanczos, E., Schöpf, V.E., Simon, J.C., 1997. High CD44 surface expression on primary tumours of malignant melanoma correlates with increased metastatic risk and reduced survival. Eur. J. Cancer 33, 926–930.

Dong, Z., 2002. The molecular mechanisms of arsenic-induced cell transformation and apoptosis. Environ. Health Perspect. 110, 757–759.

Drápela, S., Bouchal, J., Jolly, M.K., Culig, Z., Souček, K., 2020. ZEB1: A critical regulator of cell plasticity, DNA damage response, and therapy resistance. Front. Mol. Biosci. 7, 36.

Duong, H.C., Tran, L.T.T., Vu, M.T., Nguyen, D., Tran, N.T.V., Nghiem, L.D., 2021. A new perspective on small-scale treatment systems for arsenic affected groundwater. Environ. Technol. Innov. 23, 101780.

Germolec, D.R., Yoshida, T., Gaido, K., Wilmer, J.L., Simeonova, P.P., Kayama, F., Burleson, F., Dong, W., Lange, R.B., Luster, M.I., 1996. Arsenic induces overexpression of growth factors in human keratinocytes. Toxicol. Appl. Pharmacol. 141, 308–318.

Hartley, T.N., Macdonald, A.J., McGrath, S.P., Zhao, F.J., 2013. Historical arsenic contamination of soil due to long-term phosphate fertiliser applications. Environ. Pollut. 180, 259–264.

Henry, H., Naujokas, M.F., Attanayake, C., Basta, N.T., Cheng, Z., Hettiarachchi, G.H., Maddaloni, M., Schadt, C., Scheckel, K.G., 2015. Bioavailability-based in situ remediation to meet future lead (Pb) standards in urban soils and gardens. Environ. Sci. Technol. 49, 8948–8958.

Hirano, S., Watanabe, T., Kobayashi, Y., 2013. Effects of arsenic on modification of promyelocytic leukemia (PML): PML responds to low levels of arsenite. Toxicol. Appl. Pharmacol. 273, 590–599.

Huang, M., Kang, Y., Wang, W., Chan, C.Y., Wang, X., Wong, M.H., 2015. Potential cytotoxicity of water-soluble fraction of dust and particulate matters and relation to metal (loid)s based on three human cell lines. Chemosphere 135, 61–66.
Ismail, N.A., Amin, K.A.M., Majid, Razali, M.H., 2019. Gellan gum incorporating titanium dioxide nanoparticles biofilm as wound dressing: Physicochemical, mechanical, antibacterial properties and wound healing studies. Mater. Sci. Eng. C 103, 109770.
Jabłońska-Trypuć, A., 2021. Human cell culture, a pertinent in vitro model to evaluate the toxicity of landfill leachate/sewage sludge. a review. Environ. 8 (54).
Jiang, R., Li, Y., Xu, Y., Zhou, Y., Pang, Y., Shen, L., Zhao, Y., Zhang, J., Zhou, J., Wang, X., 2013. EMT and CSC-like properties mediated by the IKKβ/IκBα/RelA signal pathway via the transcriptional regulator, snail, are involved in the arsenite-induced neoplastic transformation of human keratinocytes. Arch. Toxicol. 87, 991–1000.
Konradi, S., Yasmin, N., Haslwanter, D., Weber, M., Gesslbauer, B., Sixt, M., Strobl, H., 2014. Langerhans cell maturation is accompanied by induction of N-cadherin and the transcriptional regulators of epithelial–mesenchymal transition ZEB1/2. Eur. J. Immunol. 44, 553–560.
Leal, L.T.C., Guney, M., Zagury, G.J., 2018. In vitro dermal bioaccessibility of selected metals in contaminated soil and mine tailings and human health risk characterization. Chemosphere 197, 42–49.
Li, S.-W., Liu, X., Sun, H.-J., Li, M.-Y., Zhao, D., Luo, J., Li, H.-B., Ma, L.W., 2017. Effect of phosphate amendment on relative bioavailability and bioaccessibility of lead and arsenic in contaminated soils. J. Hazard. Mater. 339, 256–263.
Liang, C.-C., Park, A.Y., Guan, J.-L., 2007. In vitro scratch assay: A convenient and inexpensive method for analysis of cell migration in vitro. Nature Protoc. 2, 329–333.
Lin, P., Guo, Y., He, L., Liao, X., Chen, X., He, L., Lu, Z., Qian, Z.J., Zhou, C., Hong, P., 2021. Nanoplastics aggravate the toxicity of arsenic to AGS cells by disrupting ABC transporter and cytoskeleton. Ecotoxicol. Environ. Safety 227, 112885.
Lin, C., Wang, J., Cheng, H., Ouyang, W., 2015. Arsenic profile distribution of the wetland argialbolls in the sanjiang plain of northeastern China. Sci. Rep. 5, 1–6.
Liu, S., Wu, B., Yu, Y., Y., Shen., 2019. Memory effect of arsenic-induced cellular response and its influences on toxicity of titanium dioxide nanoparticle. Sci. Rep. 9, 1–10.
Llorens, M.C., Rossi, F.A., García, I.A., Cooke, M., Abba, M.C., Lopez-Haber, C., Barrio-Real, L., Vaglienti, M.V., Rossi, M., Bocco, J.L., 2019. PKCα modulates epithelial-to-mesenchymal transition and invasiveness of breast cancer cells through ZEB1. Front. Oncol. 9, 1323.
Makris, K.C., Quazi, S., Nagar, R., Sarkar, D., Datta, R., Sylvia, V.L., 2008. In vitro model improves the prediction of soil arsenic bioavailability: Worst-case scenario. Environ. Sci. Technol. 42, 6278–6284.
Martinez, V.D., Becker-Santos, D., Vucic, E.A., Lam, S., Lam, W.L., 2011. Induction of human squamous cell-type carcinomas by arsenic. J. Skin Cancer 454157. http://dx.doi.org/10.1155/2011/454157.
Meng, Z.Q., Meng, N.Y., 2000. Effects of arsenic on blast transformation and DNA synthesis of human blood lymphocytes. Chemosphere 41, 115–119.
Mesrati, M.H., Syafruddin, S.H., Mohtar, M.A., Syahir, A., 2021. CD44: A multifunctional mediator of cancer progression. Biomolecules 11, 1850.
Mia, M.M., Singh, M.K., 2019. The hippo signaling pathway in cardiac development and diseases. Front. Cell Dev. Biol. 7, 211.
Ngalame, N.N.O., Tokar, E.J., Person, R.J., Xu, Y., Waalkes, M.P., 2014. Aberrant microRNA expression likely controls RAS oncogene activation during malignant transformation of human prostate epithelial and stem cells by arsenic. Toxicol. Sci. 138, 268–277.
Palma-Lara, I., Martínez-Castillo, M., Quintana-Pérez, J., Arellano-Mendoza, M.G., Tamay-Cach, F., Valenzuela-Limón, O.L., García-Montalvo, E.A., Hernández-Zavala, A., 2020. Arsenic exposure: A public health problem leading to several cancers. Regul. Toxicol. Pharmacol. 110, 104539.
Pathania, Y.S., 2021. Mottled pigmentation, palmar keratosis and chronic arsenic poisoning. QJM: Internatl. J. Med. 114, 265–266.
Pijuan, J., Barceló, C., Moreno, D.F., Maiques, O., Sisó, P., Marti, R.M., et al., 2019. In vitro cell migration, invasion, and adhesion assays: From cell imaging to data analysis. Front. Cell Dev. Biol. 7, 107.
Pillai-Kastoori, L., Schutz-Geschwender, A.R., Harford, J.A., 2020. A systematic approach to quantitative Western blot analysis. Anal. Biochem. 593, 113608.
Primeaux, M., Gowrikumar, S., Dhawan, P., 2022. Role of CD44 isoforms in epithelial-mesenchymal plasticity and metastasis. Clin. Exp. Metastasis 39 (3), 391–406.
Quazi, S., Sarkar, D., Datta, R., 2010. Effect of soil aging on arsenic fractionation and bioaccessibility in inorganic arsenical pesticide contaminated soils. Appl. Geochem. 25, 1422–1430.
Rahman, M.S., Clark, M.W., Yee, L.H., Burton, E.D., 2019. Arsenic (V) sorption kinetics in long-term arsenic pesticide contaminated soils. Appl. Geochem. 111, 104444.
Rajwar, Y.C., Jain, N., Bhatia, G., Sikka, N., Garg, B., Walia, E., 2015. Expression and significance of cadherins and its subtypes in development and progression of oral cancers: A review. J. Clin. Diagnos. Res. 9 (5), ZE05-7.
Rakhimbekova, S., O'Carroll, D.M., Robinson, C.E., 2021. Occurrence of arsenic in nearshore aquifers adjacent to large inland lakes. Environ. Sci. Technol. 55, 8079–8089.
Ribatti, D., Tamma, R., Annese, T., 2020. Epithelial-mesenchymal transition in cancer: A historical overview. Transl. Oncol. 13 (6), 100773.
Ruan, W., Lai, M., 2007. Actin, a reliable marker of internal control? Clin. Chim. Acta 385 (1–2), 1–5.
Sánchez-Tilló, E., Siles, L., De Barrios, O., Cuatrecasas, M., Vaquero, E.C., Castells, A., Postigo, A., 2011. Expanding roles of ZEB factors in tumorigenesis and tumor progression. Am. J. Cancer Res. 1 (7), 897.
Sanyal, T., Paul, M., Bhattacharjee, S., Bhattacharjee, P., 2020. Epigenetic alteration of mitochondrial biogenesis regulatory genes in arsenic exposed individuals (with and without skin lesions) and in skin cancer tissues: A case control study. Chemosphere 258, 127305.
Sarkar, D., Datta, R., 2003. A modified in-vitro method to assess bioavailable arsenic in pesticide-applied soils. Environ. Pollut. 126 (3), 363–366.
Schneider, C.A., Rasband, W.S., Eliceiri, K.W., 2012. NIH image to ImageJ: 25 years of image analysis. Nature Methods 9 (7), 671–675.
Senbanjo, L.T., Chellaiah, M.A., 2017. CD44: a multifunctional cell surface adhesion receptor is a regulator of progression and metastasis of cancer cells. Front. Cell Dev. Biol. 5, 18.
Shavit, E., Shavit, E., 2010. Lead and arsenic in morchella esculenta fruitbodies collected in lead arsenate contaminated apple orchards in the northeastern United States: A preliminary study. Fungi Mag. Spring 3 (2), 11–18.
Sidhu, V., Sarkar, D., Datta, R., 2016. Effects of biosolids and compost amendment on chemistry of soils contaminated with copper from mining activities. Environ. Monit. Assess. 188 (3), 1–9.
Singh, K., Sinha, M., Pal, D., Tabasum, S., Gnyawali, S.C., Khona, D., et al., 2019. Cutaneous epithelial to mesenchymal transition activator ZEB1 regulates wound angiogenesis and closure in a glycemic status–dependent manner. Diabetes 68 (11), 2175–2190.
Sodhi, K.K., Kumar, M., Agrawal, P.K., Singh, D.K., 2019. Perspectives on arsenic toxicity, carcinogenicity and its systemic remediation strategies. Environ. Technol. Innov. 16, 100462.
Straif, K., Benbrahim-Tallaa, L., Baan, R., Grosse, Y., Secretan, B., El Ghissassi, F., et al., 2009. A review of human carcinogens–part C: Metals, arsenic, dusts, and fibres. Lancet Oncol. 10 (5), 453–454.
Surdu, S., Fitzgerald, E.F., Bloom, M.S., Boscoe, F.P., Carpenter, D.O., Haase, R.F., et al., 2013. Occupational exposure to ultraviolet radiation and risk of non-melanoma skin cancer in a multinational European study. PLoS One 8 (4), e62359.
Teng, Y., Fan, Y., Ma, J., Lu, W., Liu, N., Chen, Y., et al., 2021. The PI3k/Akt pathway: Emerging roles in skin homeostasis and a group of non-malignant skin disorders. Cells 10 (5), 1219.

Tessier, A., Campbell, P.G., Bisson, M., 1979. Sequential extraction procedure for the speciation of particulate trace metals. Anal. Chem. 51 (7), 844–851.
Thacker, J.S., Yeung, D.H., Staines, W.R., Mielke, J.G., 2016. Total protein or high-abundance protein: Which offers the best loading control for Western blotting? Anal. Biochem. 496, 76–78.
Thang, N.D., Yajima, I., Kumasaka, M.Y., Kato, M., 2014. Bidirectional functions of arsenic as a carcinogen and an anti-cancer agent in human squamous cell carcinoma. PLoS One 9 (5), e96945.
Truskey, G.A., 2018. Human microphysiological systems and organoids as in vitro models for toxicological studies. Front. Public Health 6, 185.
Udensi, U.K., Graham-Evans, B.E., Rogers, C., Isokpehi, R.D., 2011. Cytotoxicity patterns of arsenic trioxide exposure on HaCaT keratinocytes. Clin. Cosmet. Investig. Dermatol. 4, 183.
Van Norman, G.A., 2019. Limitations of animal studies for predicting toxicity in clinical trials: Is it time to rethink our current approach? JACC Basic Transl. Sci. 4 (7), 845–854.
Walter, M.N., Wright, K.T., Fuller, H.R., MacNeil, S., Johnson, W.E.B., 2010. Mesenchymal stem cell-conditioned medium accelerates skin wound healing: An in vitro study of fibroblast and keratinocyte scratch assays. Exp. Cell Res. 316 (7), 1271–1281.
Wang, Z., Yang, J., Fisher, T., Xiao, H., Jiang, Y., Yang, C., 2012. Akt activation is responsible for enhanced migratory and invasive behavior of arsenic-transformed human bronchial epithelial cells. Environ. Health Perspect. 120 (1), 92–97.
Weinmuellner, R., Kryeziu, K., Zbiral, B., Tav, K., Schoenhacker-Alte, B., Groza, D., et al., 2018. Long-term exposure of immortalized keratinocytes to arsenic induces EMT, impairs differentiation in organotypic skin models and mimics aspects of human skin derangements. Arch. Toxicol. 92 (1), 181–194.
Xue, S., Shi, L., Wu, C., Wu, H., Qin, Y., Pan, W., et al., 2017. Cadmium, lead, and arsenic contamination in paddy soils of a mining area and their exposure effects on human HEPG2 and keratinocyte cell-lines. Environ. Res. 156, 23–30.
Yang, M.-H., Li, B., Chang, K.-J., 2022. Notch pathway inhibition mediated by arsenic trioxide depletes tumor initiating cells in small cell lung cancer. Mol. Biol. Rep. 1–9.
Yi, Y., Xie, H., Xiao, X., Wang, B., Du, R., Liu, Y., et al., 2018. Ultraviolet a irradiation induces senescence in human dermal fibroblasts by down-regulating DNMT1 via ZEB1. Aging 10 (2), 212.
Zhang, P., Sun, Y., Ma, L., 2015. ZEB1: At the crossroads of epithelial-mesenchymal transition, metastasis and therapy resistance. Cell Cycle 14 (4), 481–487.
Zhao, C.Q., Young, M.R., Diwan, B.A., Coogan, T.P., Waalkes, M.P., 1997. Association of arsenic-induced malignant transformation with DNA hypomethylation and aberrant gene expression. Proc. Natl. Acad. Sci. 94 (20), 10907–10912.
Zhou, Q., Jin, P., Liu, J., Li, S., Liu, W., Xi, S., 2021. HER2 overexpression triggers the IL-8 to promote arsenic-induced EMT and stem cell-like phenotypes in human bladder epithelial cells. Ecotoxicol. Environ. Safety 208, 111693.